Self-healing coatings: an alternative route for anticorrosion protection

Valérie Sauvant-Moynot, Serge Gonzalez, Jean Kittel

Self-healing coatings: an alternative route for anticorrosion protection

Valérie Sauvant-Moynot, Serge Gonzalez, Jean Kittel
IFP Lyon – BP3 – 69390 Vernaison (France)
valerie.sauvant@ifp.fr

Abstract
Polymer coating systems are classically applied on a metal surface to provide a dense barrier against the corrosive species. Cathodic protection is used for many applications at the same time than coatings to protect the metal structures from corrosive attack when the coating is damaged. However, the current demand will increase with the disbonded areas; moreover, the reactions that take place at the cathode can cause a progressive enlargement of the unbonded area. Self-healing coatings were considered as an alternative route for efficient anticorrosion protection while maintaining a low demand in cathodic protection. Such coatings typically incorporate micro or nanocapsules that contain film-formers and repair the coating damage when the coating is scratched. Self-healing systems were developed for metal structures under cathodic protection using specific-film formers sensitive to the electrical field and pH encountered in the vicinity of a default on a coated structure under cathodic protection. The present paper describes the principle of this novel self-healing concept and discusses the healing efficiency on the basis of laboratory results. Electrochemical Impedance Spectroscopy was used to evaluate the performance of the barrier efficiency and continuous current demand monitoring assessed the ability of specific film-formers to provide self-healing and repair defects generated through the coating to the metal.

1. Introduction

Corrosion of steel causes substantial financial losses and requires tremendous efforts to limit its impact. For pipeline systems for example, uncontrolled corrosion could induce leaks, fire and explosion among others consequences. Hence selecting effective and economical techniques for minimizing the effects of corrosion is a critical design decision. Classical methods used to reduce the rate of corrosion are cathodic protection (CP), barrier protection (coatings) and passivation (anodic protection).
Cathodic protection is one of the oldest methods of anticorrosion protection [1]. An ideal CP system will maintain the neat metal surface to a potential sufficiently negative to prevent the metal structures from corrosive attack in a given medium. Hence cathodic reactions occurring on the metal surface in contact with a corrosive environment and depending of the potential are:

$$O_2 + 2H_2O + 4e^- \rightarrow 4\ OH^- \quad (1)$$

$$2H^+ + 2e^- \rightarrow H_2 \quad (2)$$

$$2H_2O + 2e^- \rightarrow 2OH^- + H_2 \quad (3)$$

with protons or water reduction occurring in case of highly negative potentials (< -1.0 $V/_{Ag/AgCl}$). Impressed current or sacrificial anodes are applied to achieve cathodic protection of a metal structure.
The use of polymer coating systems applied on a metal surface is an interesting solution to provide a dense barrier against the corrosive species and post-pone their ingress to the metal surface. The protection effectiveness of a coating is closely tied to the quality of the applied coating and depends mainly on applications parameters (surface preparation, conditions of application and coating thickness) but also on the coating adhesion to steel. But barrier properties are also governed by the coating permeability towards corrosive species which is an intrinsic property [2-4].

Passivation is another form of anticorrosion protection which occurs when a passive oxide layer forms on the exposed area. The concept of passive oxide formation is based on the anodisation of an active metal by a redox reaction, whereby an active metal with lower standard potential becomes oxidised in the presence of a cathodic reaction with higher standard potential. The protective activity of polyanyline (conducting polymer in its oxidised form) towards metal surface is attributed to the formation of a passive layer with concomitant partial reduction of the polymer [5-7].

Improvement of the anticorrosion protection can be obtained by combining classical protection methods together. It was reported that performance of polyaniline/epoxy two-coated system on steel was superior to that of epoxy coating alone [8]. Besides, it is well known that the combined use of CP system and barrier coatings offers many benefits: when the coating is damaged to the metal, the CP system will protect the bare metal from corrosive attack; in turn, the less conductive the coating, the smaller the amount of current needed for CP, allowing CP to be applied less expensively. However, the overall cathodic protection current demand will increase with the coating defect areas, which dictates the operational costs associated with the use of a CP system. Coating defects can be caused by mishandling or misuse of the coated structure, which may be a buried or immersed pipeline, a boat, an offshore platform.... In the case of external pipeline coatings, they are frequently damaged during handling and installation of the pipe, or are the result of rock damage during backfill. In many cases, it is assumed that initial damage to the coating is inevitable, and the cathodic protection system is designed in consequence. However, cathodic protection might also play a negative role by enlarging pre-existing defects, due to the production of hydroxides at the cathode (local alkalinisation) and the release of hydrogen [9]. This phenomenon is often referred to as "cathodic disbondment". The actual generation of hydrogen gas takes place only at fairly high negative potentials but, under rare conditions, it could literally strip off a coating in a matter of hours whereas hydrogen production may cause hydrogen embrittlement in the metal. Thus, either cathodic effects (hydroxyl and possible hydrogen production) leading to cathodic disbondment that adversely affects a coating are obviously a limitation of the combined use of a CP system with an organic coating.

'Smart' coatings can be considered as an alternative route to further improve the corrosion protection of metals. Smart coatings are engineered to provide a superior resistance to corrosion on demand when, for example, the coating is breached or stressed (mechanically or chemically) or when an electrical or mechanical control signal is applied to the coating. For example, the introduction of calcium alumina fillers into polyphenylenesulfide coatings was identified as an efficient method to seal and repair microcracks generated during exposure to hydrothermal environment at 200°C [10]. When microcracks occur, calcium alumina fillers were reported to disclose in the grooves of the coating and lead to the rapid formation of crystalline products by both carbonation and decalcification-hydration reactions occurring in contact with hot CO_2-laden brine. Those crystals revealed to play an essential role in reconstituting and restoring the function of the failed coating as corrosion-preventing barrier. Besides, smart corrosion inhibition coatings will generate or release an inhibitor only when necessary in case of corrosion initiation. Kendig et al [11-12] proposed to build chemical or nano-structures into a protective coating such that corrosion reaction drives the release of a corrosion inhibitor using suitably doped polyaniline coatings on aluminium exposed to salt fog environment. Other works have focused on dispersing inhibitor or sealant-containing vesicles that break open to release an inhibitor or a sealant when experiencing a mechanical or chemical stress. The addition of

microencapsulated materials within a fusion bonded epoxy (FBE) coating was presented as a novel technique to design a more damage tolerant FBE coating than traditional ones [13]: the mechanical damage which weakens conventional coatings instead ruptures the microcapsules which in turn release their protective fill and "heal" the FBE coating, preserving its barrier properties. The self-healing concept where curable healing agents are stored in containers dispersed throughout a polymer matrix was investigated first with single component healants [14], then two components ones by White et al [15-16]: in that particular case, the healing agent released by urea formaldehyde (UF) microcapsule breakage contacts an embedded catalyst triggering a ring-opening metathesis polymerisation that effectively bonds the crack faces closed. The efficiency of a self-healing corrosion protection coating system using UF microcapsules containing several types of film forming compounds (healants) and corrosion inhibitors mixed into commercially available coating systems has been extensively investigated for use in coatings on outdoor steel by Kumar et al [17-20] or for use in epoxy composites [21]. Recently, the use of layer-by-layer deposited polyelectrolytes as nanocontainers for a corrosion inhibitor in anticorrosion coatings was successfully investigated as a new approach for the formation of smart self-healing anticorrosion coatings [22].
In the present study, attempts were made to develop improved self-healing coatings dedicated to the anticorrosion protection of metal structures under cathodic protection. Based upon the information described above, emphasis was on assessing the potential of novel self-healing agents to be microencapsulated. Specific film-formers under investigation [22] were selected and developed for their sensitivity to both the electrical field and the alkaline pH encountered in the vicinity of a default on a coated structure under cathodic protection (Figure 1):

- water soluble inorganic salts prone to scale deposition at the metal surface under cathodic potential;
- water soluble and self-curable cathodically electrodepositable polymer adducts.

In this paper specific film-formers are called, respectively, inorganic agents and organic agents.
The factors to be assessed included the ability of specific films formers mixed in a commercial coating to reduce the demand in cathodic current after damage, to minimise the risks of cathodic disbondment initiated at the steel / coating interface in place of a coating damage, and to efficiently heal a crack. The experimental study was based on the continuous monitoring of the cathodic current demand and on electrochemical impedance spectroscopy (EIS) used to evaluate the barrier properties of coatings.

2. Experimental

2.1 Preparation of inorganic agents

Magnesium ions Mg^{2+} were selected in this work as potentially active agents to be investigated because they react with hydroxyl ions in alkaline environment and precipitate into magnesium hydroxyde when the interfacial pH reaches the critical value of 9.3 [23]:

$$Mg^{2+} + 2OH^- \rightarrow Mg(OH)_2 \quad (4)$$

The encapsulation of a solution of magnenium sulfate $MgSO_4$ was the first step of the preparation stage. Microencapsulation is a technique through which liquid materials either aqueous or non-aqueous in nature are encapsulated within a solid shell between a

few µm to 200 µm in size [24]. The nature of shell wall material is function of the material to be encapsulated, the coating application process and the desired stimulus to rupture the capsule (impact, pH etc). In the present case, the classical UF microencapsulation process could not be used since the specific filler materials under consideration are water soluble. Choice was made to prepare epoxy-amine microcapsules because they would easily incorporate into epoxy based coatings, promptly break due to the good adhesion between matrix and microcapsules [25] and efficiently release their filler materials once damaged due to the intrinsic fragility of epoxy shells. This damage may be the result of an impact to the coating or a crack during possible bending.

Epoxy-amine microcapsules were prepared by interfacial reaction in inverse emulsion as illustrated in Figure 2. An aqueous solution was prepared by mixing 2 g of $MgSO_4$, 3 g of aliphatic diamine monomers (HY2954 from Hunstman) and 0.2 g of imidazole catalyst in 15 g water. 0.2g of acetic acid was added to maintain the solution homogeneous with a pH around 8.5 [26]. An organic solution was prepared by solving 9.8 g of Diglycidyl Ether of bisphenol-A (LY556, M_W = 380 g/mol purchased from Huntsman) and 1 g of emulsion stabilisator in API fuel (T boiling = 250°C-350°C). Then the water based solution was added to the organic solution at room temperature under thorough stirring (500 rpm), forming a stable inverse emulsion (water in oil). Interfacial reactions between resin and hardener monomers dissolved in stoichiometric composition were allowed to occur by heating the inverse emulsion to 80°C during 20 minutes under continuous agitation. Then mixture was cooled to room temperature and 1.4 g of microcapsules were collected by a first filtering, corresponding to 4.5 % output in weight. In order to improve this result, 5 g of hydrophilic silica powder (Syloid ED3 from Grace) were added to the emulsion to ease the filtering of the capsules and avoid their agglomeration. 24g of microcapsules were collected by a second filtering, increasing the global output to 81.0 % in weight.

The obtained microcapsules were ranging in size from 10 µm to 240 µm diameter, as shown by optical microscopy observations (Figure 3). The thermo-gravimetric analysis revealed an average water content reaching 10 % in weight, according to the weight loss accompanying the 1 hour heating step at 120°C (Figure 4). Since $MgSO_4$ was initially dissolved in water, one can estimate from the initial ratio of salt to water content that microspheres contain about 1.4 % of $MgSO_4$. The presence of $MgSO_4$ in the encapsulated solution was confirmed after the calcination of microspheres in an oven at 650°C for 4 hours, washing of the inorganic residue by deionised water to dissolve the salt, filtering and precipitation of $BaSO_4$ when adding a few drops of $Ba(NO_3)_2$ concentrate solution. As a conclusion, the encapsulation process was successful but its efficiency may be improved in the future.

2.2 Preparation of organic agents

The principle of water soluble and self-curable epoxy electrodepositable adducts was already described by Kumar et al [27] to ease the cataphoretic paint process. These adducts are epoxy-functionalised monomers neutralised by acetic acid to form a water soluble acetate adduct prone to electrophoresis under an applied voltage ranging from 5V to 240 V (equation 5). At the cathode, the ammonium form of the functionalised adduct reacts with hydroxyls anions and deposes as a film (equation 6). Then self-cure of the adduct having epoxy and tertiary amino groups proceeds by anionic polymerisation at room temperature initiated by the tertiary groups (equations 7 and 8):

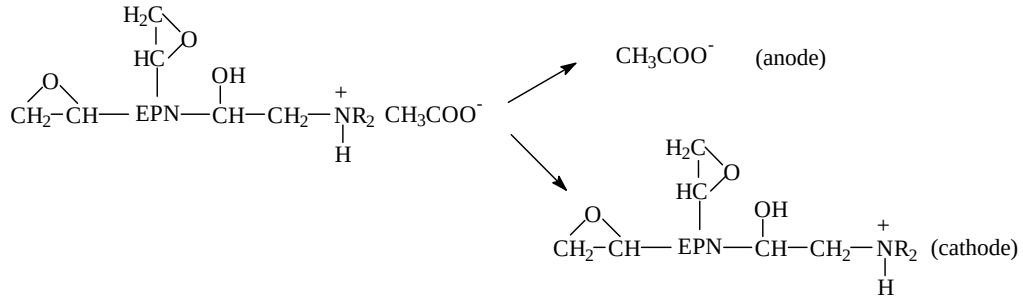

(5)

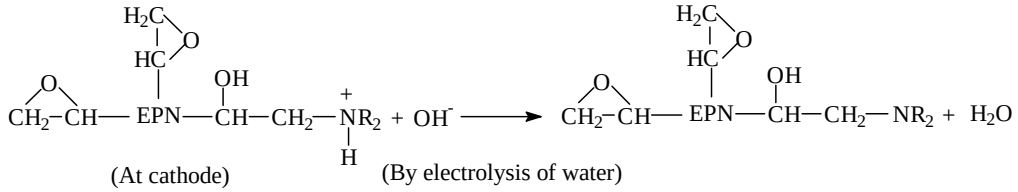

(6)

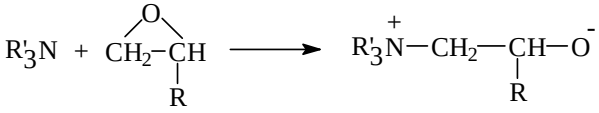

(7)

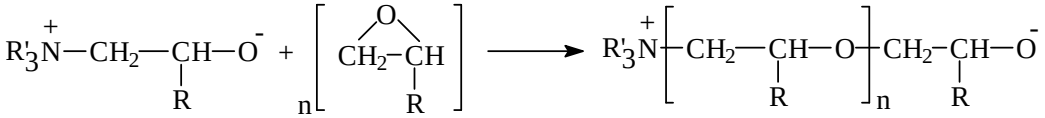

(8)

In this work, organic film-former agents were prepared by an original process avoiding the encapsulation stage. In a first step, epoxidised phenol-novolac polyepoxide resin (EPN 1138 from Araldite with an epoxy functionality of 3.6) solubilised in 2-methoxy ethanol (50 %, wgt.) was mixed with diethanol amine (DEtOA from Huntsman) in non stoichiometric proportions (1/1.7 moles epoxy/amine ratio). The mixture was allowed to react during 24 hours at 30°C to produce the epoxy functionalised EPN-tertiary amine adduct (water insoluble). In a second step, the adduct was neutralised by acetic acid to get a water soluble acetate adduct suitable for use in cathodic electrodeposition. In a third step, the acetate adduct was dried to evaporate water and a fine white and very brittle powder was collected. These organic grains with average diameter of 30 ± 10 µm (Figure 5) were thought to be very attractive for use as self-repairing fillers because they can be easily incorporated into a polymer matrix, avoiding the encapsulation step. When the grain's surfaces come in contact with water diffusing into a crack, hydration is expected to occur and allow the migration of the acetate adduct to the cathode, deposition and self-cure as previously described in equations 5 to 9.

2.3 Coating composition and preparation

Coatings investigated in this study were based on commercial liquid epoxy-amine paint (Eurokote 450 supplied by BS Coatings) chosen for its cure at low temperature. Reference coats were made out of cross-linked monomers used as received and mixed at stoichiometric composition. Prior to coating, low carbon steel panels (60*100*3 mm^3) were freshly sand-blasted to a near-white metal finish in accordance with ISO 8501-01. The steel roughness was evaluated according to ISO 8503-2 to R_{ZD} = 30µm. Epoxide-

amine mixtures containing up to 30%(wt.) of fillers were prepared at room temperature and carefully applied on steel panels with a "Baker" type filmograph in a single operation in order to obtain a flawless coating after 3 days cure at ambient temperature. Coating dry film thickness (DFT) was controlled using a magnetic thickness gauge. Specimens were stored in silica-gel desiccators.

2.4 Electrodeposition cell

The electrodeposition cell consisted of a glass baker of 200ml capacity having 150ml of adduct solution. The anode of the cell was made of a graphite rectangular plate with a size equal to that of the metallic panel to be coated and that was used as the cathode. The graphite plate and the metallic panel were hung immersed in the solution up to an equal length, so as to have equal active areas (~ 20 cm^2) of both electrodes during deposition. The anode and cathode were connected to the respective terminals of a commercial potentiostat. An Ag/AgCl/KCl (sat.) reference electrode (+197 mV/SHE) was also connected to the potentiostat. Two potentials were compared for electrodeposition to the steel plate: -0.85 V vs. Ag/AgCl/KCl(sat), which represent a situation of normal cathodic protection or -1.5 V vs. Ag/AgCl/KCl(sat), corresponding to cathodic overprotection.

2.5 Electrochemical testing

Coated specimens were placed in a glass cell as pictured in Figure 6. A 1 % (wt.) NaCl aerated solution was added and the sample was polarised at a potential ranging from -0.85 V to -1.5 V vs. Ag/AgCl//KCl(sat) reference electrode. On demand, an artifical defect was intended with a cutter in the centre of the coated panel (typical dimension of the defect were a few mm long and with a groove width taken equal to 200µm). During the whole test period, the current demand for cathodic protection was recorded each 20 minutes. Periodic electrochemical impedance spectra (EIS) were also recorded throughout the entire testing. EIS measurements were done with a Gamry™ Instruments CMS 300 and a PC4/300 potentiostat. The scanning frequency range was from 100 kHz to 100 mHz with an imposed voltage amplitude of 100 mV (rms). Tests were carried out in isothermal conditions from 23°C up to 60°C to simulate the case of a coated pipe conveying warmer effluents. Exposed surface areas were ranging from 12.5 cm^2 to 75 cm^2, depending on the coating thickness. In the case of intact coatings with high impedance, enlarging the exposed area to electrolyte is a method to keep a good sensitivity in EIS measurements for thicker coating (ISO 16773).

3. Results

3.1 Reference coating

The behaviour of the reference coating has been investigated by EIS measurements performed on an intact paint (DFT 550 µm) during a few days immersion in NaCl-1% at 40°C under cathodic protection (-1.1 $V_{/Ag/AgCl}$). The evolution of the impedance modulus and phase is plotted versus frequency on Figure 7 after 0, 12, 98 and 500 hours. Bode plots in the initial stage of immersion reveal an almost capacitive behaviour over the frequency range under consideration. The drop of the impedance modulus accompanied with an increase of the phase angle in the low frequency range after a few hours immersion point out the Tg depression induced by the network plasticization by water molecules. The impedance modulus values at 0.1 Hz after 100

and 500 hours reflect the barrier properties of the coating at saturation in NaCl-1 % at 40°C. An efficient protection against corrosion is expected from this reference coating exhibiting a film resistance higher than 100 Mohm.cm^2 in the plasticized state as determined from the plateau in Bode-plot scans that occurred in low frequency regions.

Attention was also focused on the current demand related to freshly scratched reference coatings submitted to cathodic protection. The evolution with time of the current density is illustrated on Figure 8 for reference coated panels (DFT 200 µm) immersed in NaCl-1 % solution at 20°C under -0.85 V and -1.5 V/$_{Ag/AgCl}$ cathodic protection. Coatings were scratched in situ just after immersion. The defect area has been taken as constant for calculating current density values (i.e. the current density is related to the estimated area of the defect, rather than to the whole exposed area) at a given time. It is clear from this graph that the current densities remain almost stable during the first hours whatever the polarisation level under consideration. Unchanged current level within the experience time suggests that the substrate area exposed to the electrolyte did not decrease nor enlarge itself - which would reveal some cathodic disbondment effect.

3.2 Inorganic film-formers

The behaviour of a coating filled with 30 % (wt.) microcapsules containing a solution of $MgSO_4$ (DFT 650µm) was investigated by EIS during exposition to NaCl-1 % at 40°C under cathodic protection (-1.5 V/$_{Ag/AgCl}$). A manual defect was intended in situ after 19 hours immersion. The evolution of the impedance modulus and phase versus frequency is plotted on Figure 9 after 0, 17, 19 and 285 hours. Note that the total exposed area was used for the curve normalisation in those four cases. Bode plots before intending a defect reveal a behaviour almost comparative to the reference material, namely capacitive over a broad frequency range and resistive in the low frequency range, with film resistance values taken at 0.1 Hz superior to 10^8 ohm.cm^2 but declining with exposure time due to water plasticization. This reveals that the incorporation of the microcapsules in the coating did not adversely affect its intrinsic barrier properties. In contrast, the behaviour of the freshly scratched coating is completely resistive with a pore resistance approaching 2.10^4 ohm.cm^2. Unfortunately, this value remained unchanged when the inorganic filled- coating was exposed to an additional 20 days under cathodic protection, suggesting that the penetration of electrolytes through the defect areas was not restrained (Figure 10). This is also confirmed by the flat evolution with time of the current density (Figure 11) recorded on the coated specimen after the scratch was made (normalised with the defect area). This experiment shows that there is no evidence of recovery of the coatings' function as corrosion-preventing barriers thank to the addition of microencapsulated inorganic film-formers as studied. This result suggests that the choice of Mg^{2+} as repairing agent was inappropriate to reduce the current demand and provide sealing effect. This may be due to the low concentration of the repair agent in microcapsules, but could also be related to the pH conditions which may not be alkaline enough to allow $Mg(OH)_2$ scale to form. The cathodic H_2 production may also be a factor of perturbation with respect to hydrodynamics.

3.3 Organic film-formers

As a second step of the study, the focus concentrated on organic film-formers. It was first mandatory to investigate their ability to build a film on bare steel panels placed under cathodic polarisation with voltage as low as -0.85 V/$_{Ag/AgCl}$ (in comparison to

typical voltage applied for cathodic electrodeposition ranging from 5 V to 250 V). EPN-DEtOA (1:1.7 moles) adduct, prepared at 30°C in 24 hours of reaction time, was neutralised by acetic acid to produce the electrolytic composition used for the preparation of the electrolytic solution. A bare steel panel was immersed in the electrolytic composition (adduct acetate solution of concentration 20 % in deionised water) using the electrodeposition cell, and submitted to cathodic polarisation under -0.85V/$_{Ag/AgCl}$ during three days at 20°C. A similar experiment was conducted at -1.1V/$_{Ag/AgCl}$. The variation in current density (with respect to the total area of conductive substrate immersed in the electrolytic bath) with the progress of film deposition has been presented in Figure 12. It is clear from both graphs that the current density drops during the initial period of deposition, meaning that the progress of the deposition of the adduct film (electrically non-conductive) reduced the passage of current. After the three days deposition time, the current density had almost reached steady values, called the residual current with respect to the conditions of application. It can also be concluded from both graphs that the polarisation voltage significantly influences the electrodeposition yield. Indeed, increasing the polarisation voltage markedly enhanced the current density drop and the current density values under -1.1 V/$_{Ag/AgCl}$ are one order of magnitude higher than those measured under -0.85 V/$_{Ag/AgCl}$ i.e. being the minimum voltage applied for efficient cathodic protection.

At the end of each experiment, freshly deposited film on the metallic panel was taken out of the electrolytic composition and rinsed under fresh water. Films were cured at room temperature during a 15 days period before the thickness of the dry and cured film was measured by using a magnetic film thickness gauge. As a matter of fact, a 150 µm thick film was formed under -1.1 V/$_{Ag/AgCl}$, whereas a thinner film of 35 µm was deposed under -0.85 V/$_{Ag/AgCl}$ (Figure 13). By measuring the weight of paint applied during the experiment on each panel and the surface exposed, one could evaluate the electrodeposition yield at 20°C during 3 days in each case, namely 10 mg/cm^2 under -0.85 V/$_{Ag/AgCl}$ and 24 mg/cm^2 under -1.1 V/$_{Ag/AgCl}$. This result confirmed that the electrodeposition yield increased at higher applied voltage, in agreement with the literature when applied voltage are below 25 V [27]. However, the films obtained under -1.1 V/$_{Ag/AgCl}$ was non-uniform and patchy in appearance. This was attributed to the hydrogen gas evolution at the cathode, hindering proper film deposition.

The adhesion properties were evaluated after curing the electrodeposited films for 15 days at room temperature (Figure 14). Both films showed 100 % adhesion, i.e. no square was lifted by the cross-hatched test. These results were indicative of good adhesion due to the presence of a large number of hydroxyl groups per mole of adduct (6, theoretically), assessing that water soluble self-curing EPN-DEtOA based adducts are capable of electrodeposition under cathodic polarisation.

To investigate the self-healing capability of aforementioned organic agents, the current demand of a freshly scratched coating filled with 30 % (wt.) dried acetate EPN-DEtOA (1/1.7 moles) adduct (DFT 300 µm, exposition area = 20 cm^2, defect area ≈ 0.015 cm^2) was monitored with time during exposition to NaCl-1 % at 20°C under cathodic polarisation (-0.85 V/$_{Ag/AgCl}$). A similar experiment was conducted at 60°C on a freshly scratched coating filled with 30 % of organic agent (DFT 800 µm, exposition area = 14 cm^2, defect area ≈ 0.005 cm^2). The evolution of the current density with respect to the defect area is plotted versus time on the Figure 15 for both temperatures. Interestingly, the current density drops with the time whatever the temperature, which reveals that the substrate went on sealing off itself, and consequently reduced the passage of current.

Since the current demand was shown to be constant for the reference coating (i.e. without active fillers) immersed and scratched under similar conditions, this finding demonstrates that dried organic agents used as fillers in coatings under cathodic polarisation contribute to restrain the penetration of electrolytes through the defect area, and consequently reduce the demand in current. The final current density reached 3.10^{-5} mA/cm^2 at 20°C under -0.85 $V/_{Ag/AgCl}$ for the scratched coating containing organic fillers, which was one decade above the plateau value of 2.10^{-6} mA/cm^2 reached in the scratched reference coating immersed under similar conditions. This comparison indicates that the electrodeposition yield of adducts embedded in coatings is somewhat lower than when they constitute the electrolytic solution; however, progress could be expected thank to a smaller filler design and to an optimised coating formulation with respect to the defect geometry (width and volume) [28]. Kinetics of current drop was shown to be faster at higher temperature as one can expect from cathodic electrodeposition related to thermally activated diffusion process and chemical reactions. In addition, the initial current density value is higher at 60°C, reflecting the higher mobility of conductive species involved in the passage of current due to thermal activation. The microphotographs of the defect areas after cathodic electrodeposition shown on Figure 16 confirmed the growth of a film with apparent resin deposed within the scratch groove. However, it is not easy to discuss further from these pictures since the expected deposited films are transparent (clear coats).

The study then shifted to assessing the ability of the partly sealed scratched coating to protect the underlying steel against corrosion. Bode plots were obtained on the scratched coating after 40 hours exposition at 60°C under CP, 15 days curing out of the solution at ambient temperature, then immersion again for the testing (Figure 17). Bode diagrams of the scratched reference coating are also presented but defects were not similar in size, thus impedance moduli given with respect to the exposition area could not be used for comparison purpose on the contrary to the phase plots. In the low frequency region, the phase of the scratched reference coating remained fully resistive whereas the phase of the scratched coating filled with organic agents was significantly diminishing, suggesting that the formation of an organic film within the defect contributed to the barrier effect. However, impedance values remained below the outstanding properties of the intact coating, which indicates that the efficiency of organic film-formers should be further improved to get 100 % self-healing capabilities, i.e. recover initial properties.

4. Conclusions

While several general anticorrosion strategies have been reviewed, the use of self-healing polymers was investigated as a promising approach to develop smart coatings. Inorganic and organic specific film-formers were proposed and evaluated as new self-healing agents to be used in combination with cathodic polarisation. The ability to heal a crack was assessed by monitoring the evolution with time of current demand for scratched coatings containing film-formers, in comparison to a reference coating. Electrochemical impedance spectroscopy (EIS) was used to evaluate the barrier properties of coatings.

The first objective was to investigate the self-healing performance of encapsulated Mg^{2+} as inorganic film-formers which should be autonomically delivered when a crack propagates through the coating filled with capsules, ruptures the microcapsules and

releases the agents in the vicinity of the neat metal under cathodic polarisation. In the defect area, the production of hydroxyls ions should favour the formation of an inorganic deposit by precipitation of $Mg(OH)_2$. Epoxy-amine microcapsules were synthesised, ranging in diameters from 10 to 240 µm and containing 10 % in wt. of a solution of $MgSO_4$. Coatings embedding 30 % in wt. of microcapsules were prepared, cured, exposed to a solution of NaCl-1 % under cathodic protection, and manually scratched with a cutter (200 µm width) to the steel substrate. Unfortunately, no reduction of the current demand was observed, suggesting that the microcapsule size and weight fraction were not optimised with regards to the crack volume [28], or that the choice of the healing agent was not appropriate for the application. In particular, the minimum pH value required for $Mg(OH)_2$ precipitation to occur may not have been reached in our experimental conditions (small cathodic polarisation).

The second task was devoted to the evaluation of organic film-formers, namely dried water soluble and self-curable epoxy electrodepositable adducts. The encapsulation stage was avoided since agents were directly mixed in the coating as fillers (30 % in wt). Coatings after cure were exposed to NaCl-1 % under CP. After intending a manual defect in the coating using a cutter, a significant reduction in current demand was observed, assessing the self-healing ability of agents under consideration. The barrier properties were improved when compared to a scratched reference coating, even though performance after healing may still be improved by optimising the system geometry and composition with regards to the crack volume. As a main conclusion of this work, it is now possible by incorporating dried organic fillers to easily prepare self-healing coatings that are able to repair damage when used in combination with cathodic protection and maintain a low current demand.

5. Acknowledgments

The authors wish to gratefully acknowledge J. Grenier for his implication to the experimental part of this work.

6. References

[1] Roche M., Cathodic Protection: From the origins to the most recent progress, Eurocorr, 4-8 September 2005, Lisbon, Portugal

[2] Sangaj N.S. and Malshe V.C., Permeability of polymers in protective organic coatings, Progress in Organic Coatings vol.50 p.28 (2004)

[3] Sauvant-Moynot V., Duval S., Kittel J., and Lefèbvre X., Contribution to a better FBE selection for 3 layer polyolefin coatings, 16th Pipeline Protection Conference, 2-4 November 2005, Paphos, Cyprus, p.173

[4] Sauvant-Moynot V., Kittel J., Melot D., and Roche M., Three layer polyolefin coatings: how the FBE primer properties govern the long term adhesion, 17th Pipeline Protection Conference, 17-19 October 2007, Edinburgh, UK

[5] DeBerry D.W., Modification of the electrochemical and corrosion behavior of stainless steels with an electroactive coating, Journal of Electrochemical Society vol.132 p.1022 (1985)

[6] Wessling B., Schroder S., Gleeson S., Merkle H., Schroder S., and Baron F., Corrosion prevention with an organic metal (polyaniline): surface ennobling, passivation, corrosion test results, Materials and Corrosion vol.47 p.439 (1996)

[7] Schauer, T., Joos, A., Dulog, L., and Eisenbach, C. D., Protection of iron against corrosion with polyaniline primers, Progress in Organic Coatings vol.33 p.20 (1998)
[8] Tallman D.E., Pae Y., and Bierwagen G.P., Conduction Polymers and Corrosion: Polyaniline on Steel, Corrosion vol.55 p.779 (1999)
[9] Castle J.E., Cathodic Disbondment, Proceedings of the AIP Conference p.165 (1996)
[10] Sugama T and Gawlik K, Self-repairing poly(phenylenesulfide) coatings in hydrothermal environments at 200°C, Materials Letters vol.57 p.4282 (2003)
[11] Kendig M, Hon M, and Warren L, "Smart" corrosion inhibiting coatings, Progress in Organic Coatings vol.47 p.183 (2003)
[12] Kendig M and Hon M, Environmentally Triggered Release of Oxygen-Reduction Inhibitors from Inherently Conducting Polymers, Corrosion vol.60 p.1024 (2004)
[13] Enos DG, Kehr J.A., and Guilbert CR, A high-performance, damage-tolerant, fusion-bonded epoxy coating, Pipeline Protection Conference n°13 (1999)
[14] Dry C., Self repairing of composites by release of chemicals, 42nd International SAMPE Symposium, 4-8 May 1997, Anaheim, CA
[15] White D.M., Sottos N.R., Geubelle P.H., Moore J.S., Sriram S.R., Brown E.N., and Viswanathan S., Autonomic healing of polymer composites, Nature vol.409 p.794 (2001)
[16] White D.M., Sottos N.R., Geubelle P.H., Moore J.S., Sriram R., Kessler M.R., and Brown E.N., Multifunctional autonomically healing composite material, US Patent 6,518,330 B2 (2003)
[17] Kumar A. and Stephenson L.D., Self-healing coatings, Corrosion2002 paper 158, NACE International
[18] Kumar A. and Stephenson L.D., Accelerated testing of self-healing coatings, 2003, Corrosion2003 paper 221, NACE International
[19] Kumar A. and Stephenson L.D., Self-healing coatings using microcapsules and nanocapsules, Corrosion2004 paper 278, NACE International
[20] Kumar A., Stephenson L.D., and Murray J.N., Self-healing coatings for steel, Progress in Organic Coatings vol.55 p.244 (2006)
[21] Yin, Tao, Rong, Min Zhi, Zhang, Ming Qiu, and Yang, Gui Cheng, Self-healing epoxy composites - Preparation and effect of the healant consisting of microencapsulated epoxy and latent curing agent, Composites Science and Technology vol.67 p.201 (2007)
[22] Shchukin D.G., Zheludkevich M., Yasakau K., Lamaka S., Ferreira M.G., and Möhwald H., Layer-by-layer assembled nanocontainers for self-healing corrosion protection, Advanced Materials vol.18 p.1672 (2006)
[23] Deslouis C., Festy D., Gil O., Maillot V., Touzain S.., and Tribollet B., Characterisation of calcareous deposits in artificial sea water by impedances techniques: 2-deposit of Mg(OH)2 without CaCO3, Electrochimica Acta vol.45 p.1837 (2000)
[24] Ghosh S.K., Functional Coatings, chap.1, Wiley-VCH Editor (2006)
[25] Jung D., Performance and properties of embedded microspheres for self-repairing applications, PhD Thesis, University of Illinois, US (1995)
[26] Soto-Portas M.L., Argillier J-F., Méchin F., and Zydowicz N, Preparation of oil core polyamide microcapsules via interfacial polycondensation, Polymer International vol.52 p.522 (2003)

[27] Kumar P. and Trivedi M.K., Development of low-temperature self-curable water soluble polyepoxide coatings for cathodic electrodeposition, Paintindia, June 2002 p.45 (2002)
[28] Rule J.D., Sottos N.R., and White S.R., Effect of microcapsule size on the performance of self-healing polymers, Polymers vol.48 p.3520 (2007)

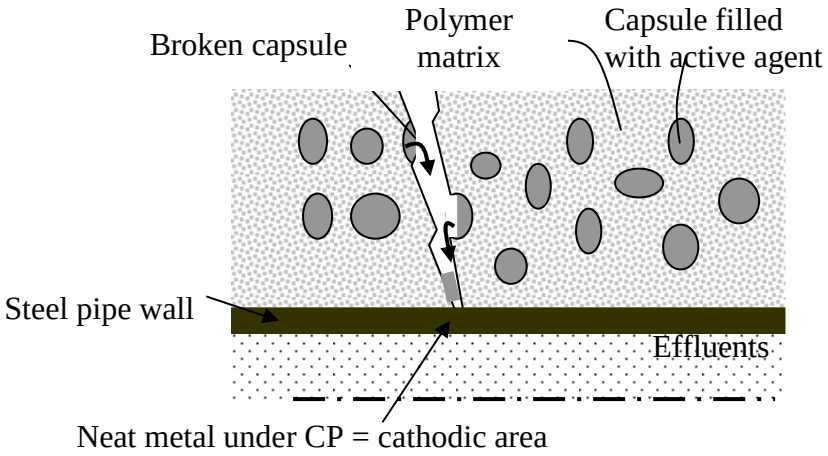

Figure 1 – Schematic illustration of the function of an organic pipe coating containing microencapsulated specific film-former agents sensitive to electrical field and pH encountered in the vicinity of cathodic areas.

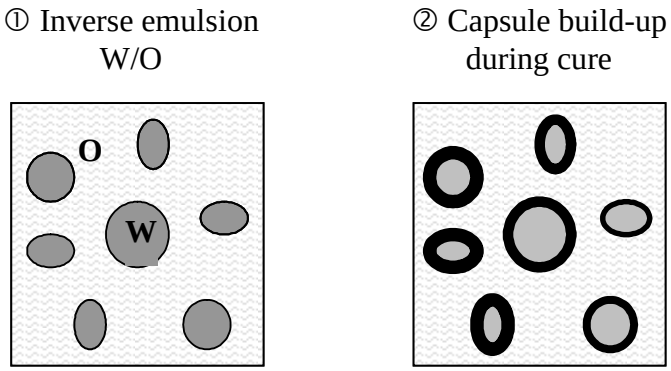

Figure 2 – Encapsulation of the inorganic agents by interfacial reaction in inverse emulsion.

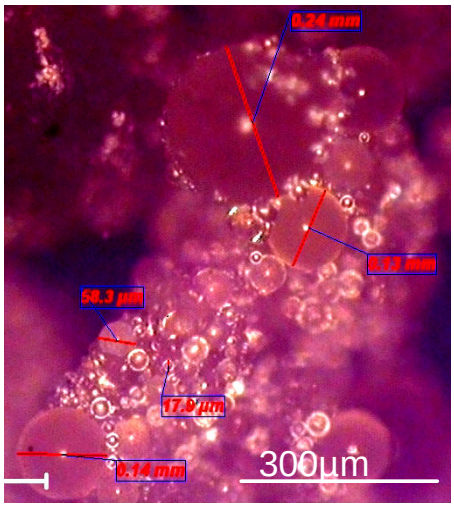

Figure 3 – Microcapsules formed by inverse emulsion in fuel API.

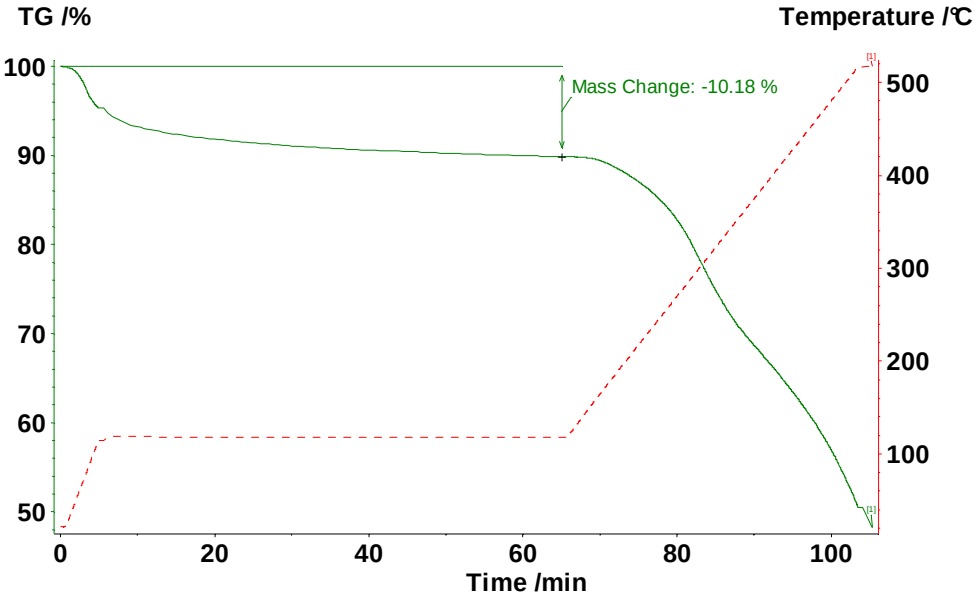

Figure 4 - Thermo-gravimetric analysis of microcapsules formed by inverse emulsion in fuel API.

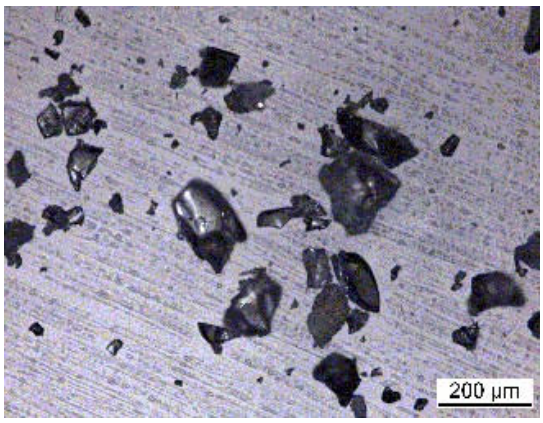

Figure 5 – Organic agent formed by drying the acetate adduct.

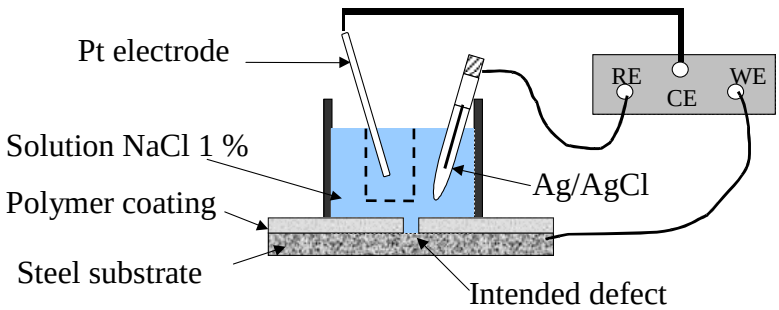

Figure 6 - Schematic of electrochemical cell used for the evaluation of the FBE coated plates under CP prior and after damage (a semi-permeable membrane is used to avoid the oxidation of chlorine ions in dichlore at the Pt electrode)

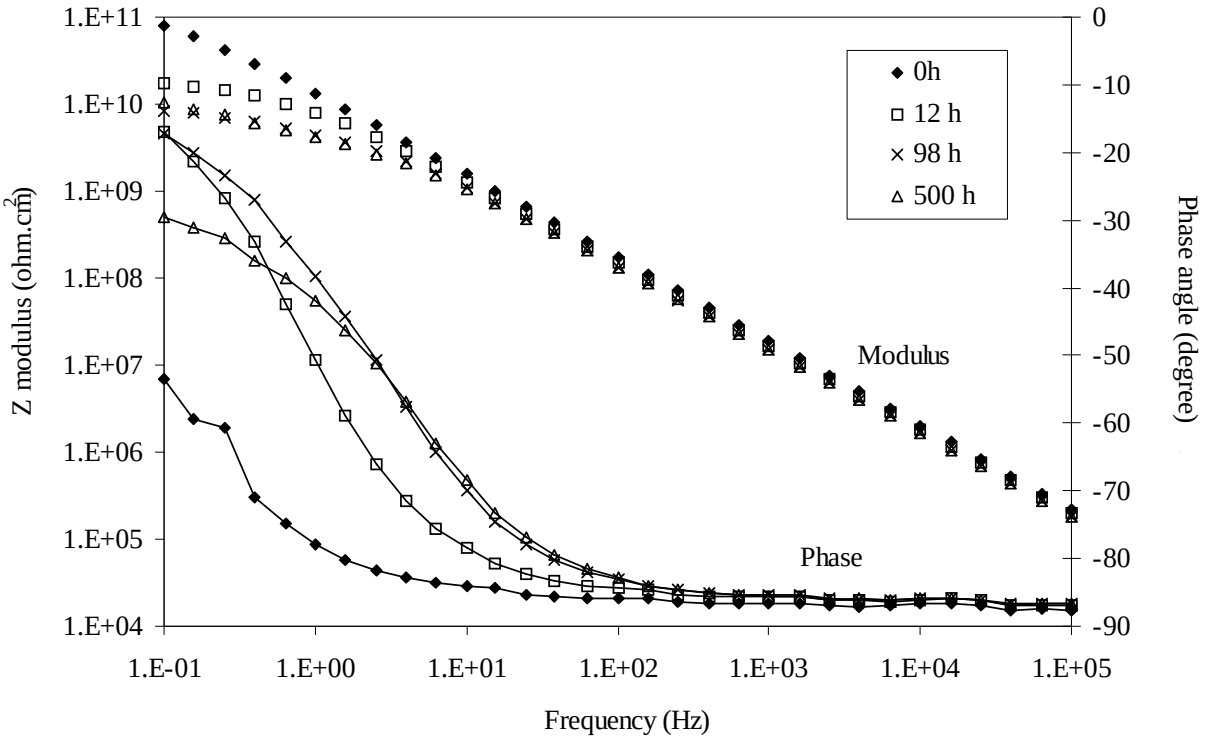

Figure 7 - Bode plots for the intact reference coating (DFT = 550 µm, exposed area = 60.5 cm^2) immersed in a solution of NaCl-1 % at 40°C under cathodic polarisation (-1.1 $V_{/Ag/AgCl}$).

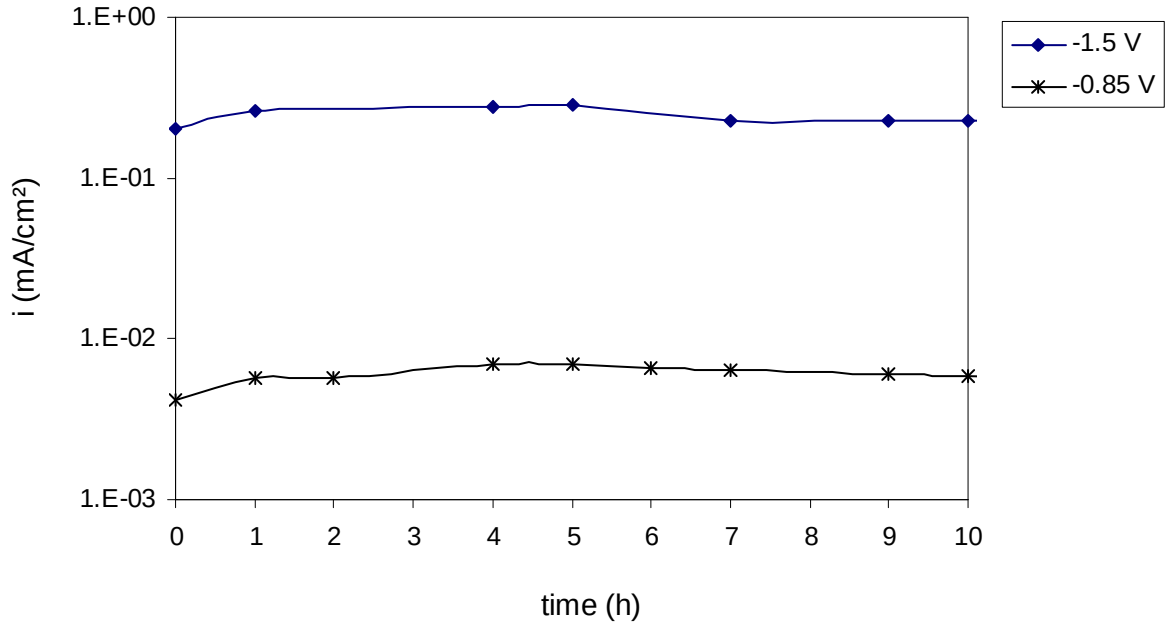

Figure 8 – Evolution of current density (with respect to defect area) with time for freshly scratched reference coatings (DFT = 200 µm, exposed areas = 14 cm^2; defect areas = 0.01 cm^2) immersed in a solution of NaCl-1 % at 20°C under cathodic polarisation (-0.85 V and -1.5 $V_{/Ag/AgCl}$).

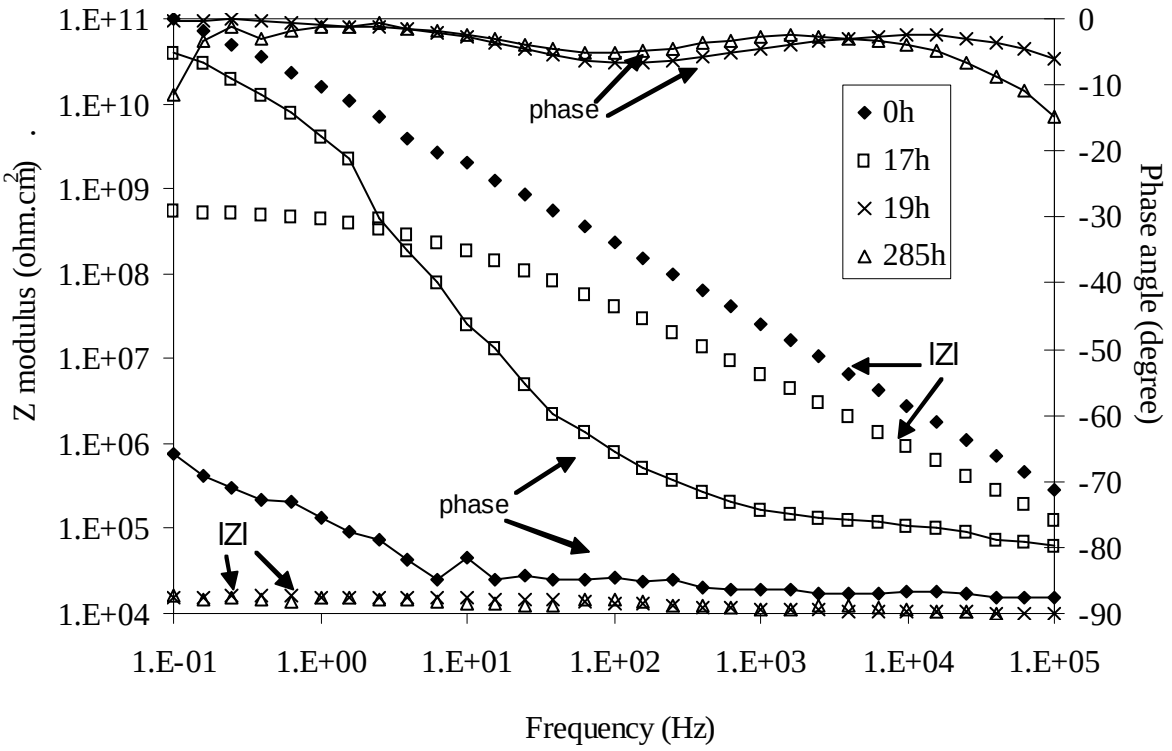

Figure 9 - Bode plots for the coating containing 30 % of inorganic film-formers (DFT = 650 µm, exposed area = 75.4 cm^2) exposed to a solution of NaCl-1 % at 40°C under cathodic polarisation (-1.5 $V_{/Ag/AgCl}$). Manual defect was intended in situ after 19 hours exposure.

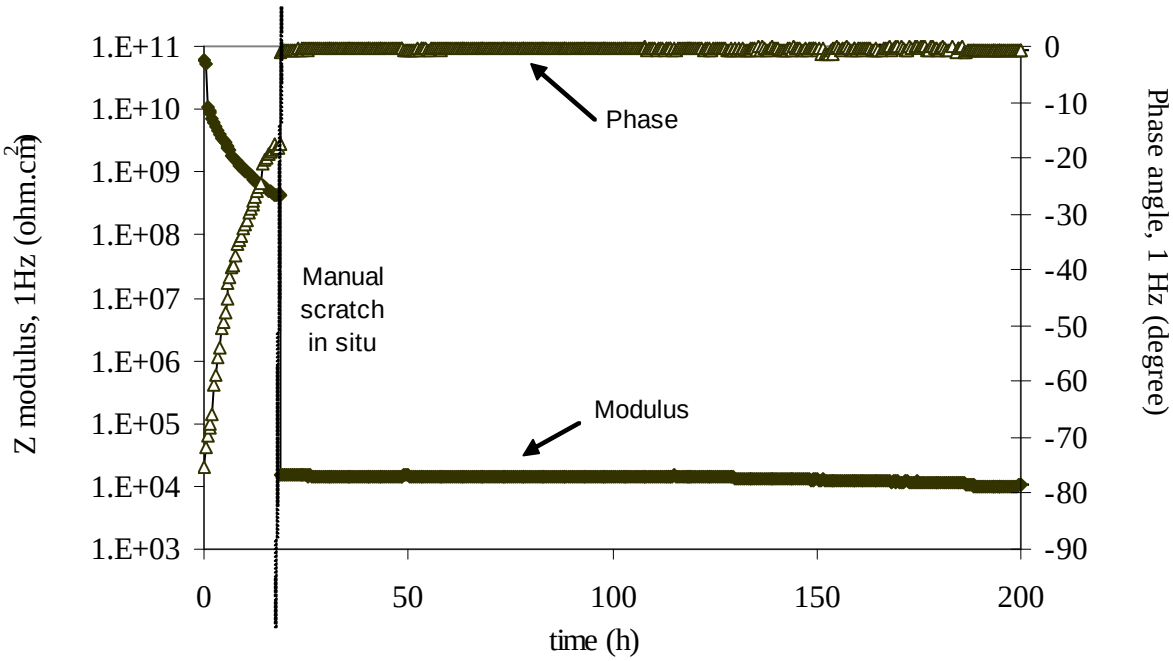

Figure 10 – Evolution with time of the impedance modulus and phase measured at 1 Hz for a coating (DFT ~ 650 µm) containing 30 % of inorganic film-formers and exposed to a solution of NaCl-1 % at 40°C under cathodic polarisation (-1.5 $V_{/Ag/AgCl}$). Manual defect was intended after in situ 19 hours exposition.

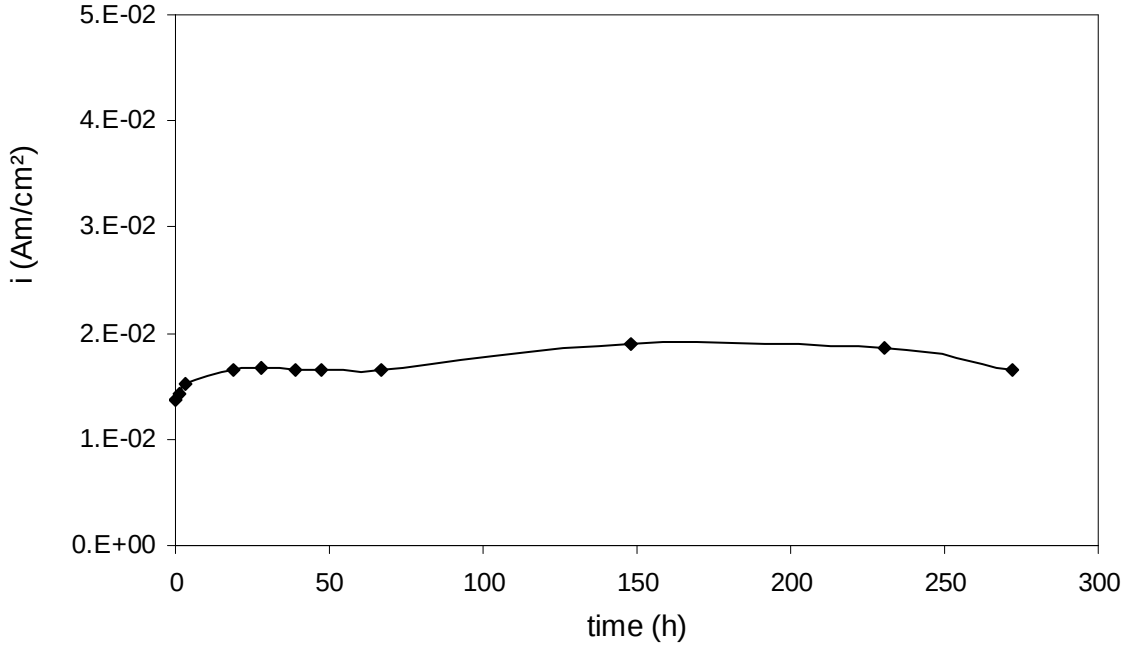

Figure 11 – Evolution of current density (with respect to defect area) with time for a freshly scratched coating containing 30 % of inorganic encapsulated agents (DFT ~ 650 µm) exposed to a solution of NaCl-1 % at 40°C under cathodic polarisation (-1.5 $V_{/Ag/AgCl}$).

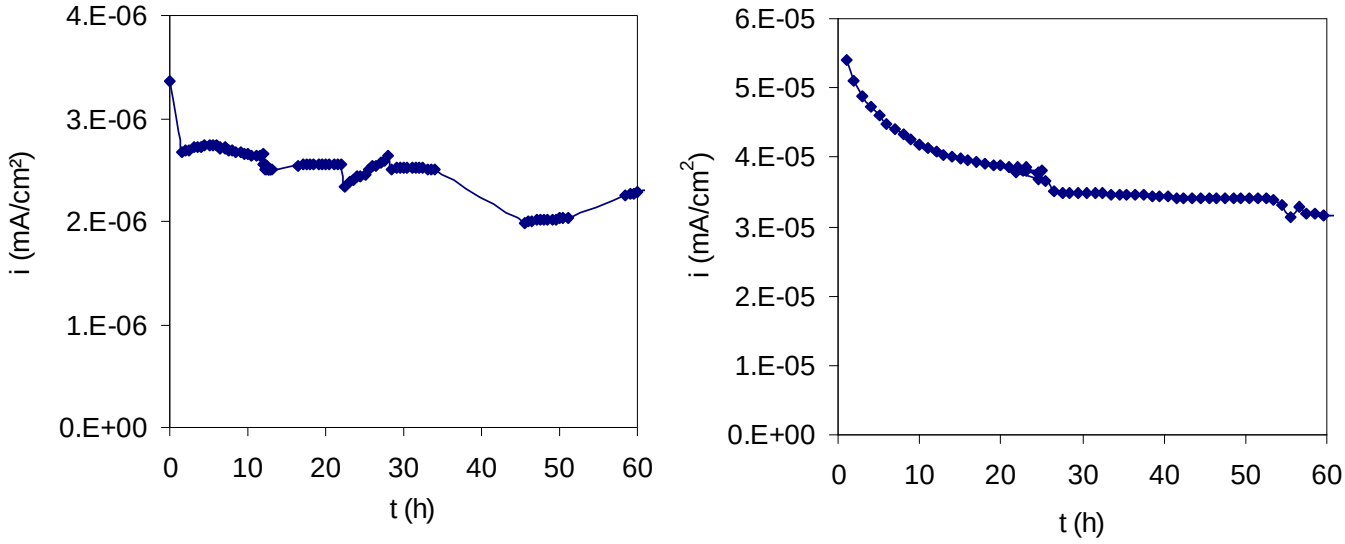

Figure 12 – Variation in current density (with respect to total exposed area) with the progress of film deposition at 20°C on bare steel panels under cathodic polarisation : -0.85 $V_{/Ag/AgCl}$ (left); -1.1 $V_{/Ag/AgCl}$ (right).

Figure 13 – Films electrodeposed on steel panels during 3 days exposure to a solution of organic film-former agents at 20°C under cathodic polarisation: -1.5 $V_{/Ag/AgCl}$ (left) ; -0.85 $V_{/Ag/AgCl}$ (right).

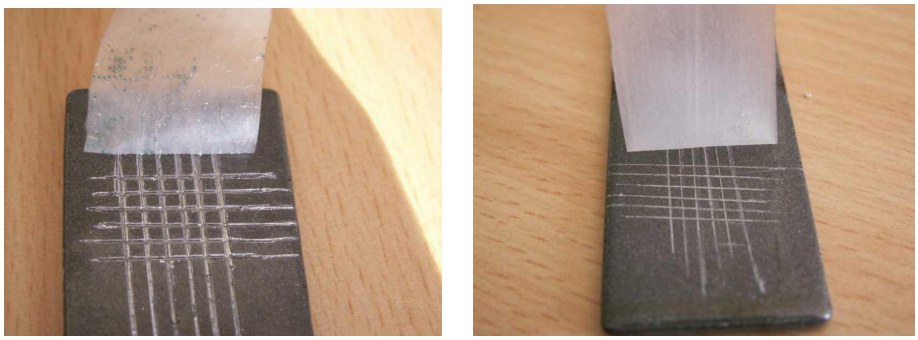

Figure 14 – Adhesion of films to steel panels measured by cross-hatch test after electrodeposition in an electrolytic bath during 3 days under cathodic polarisation and self-cure under air at room temperature during 15 days: -1.5 $V_{/Ag/AgCl}$ (left) ; -0.85 $V_{/Ag/AgCl}$ (right).

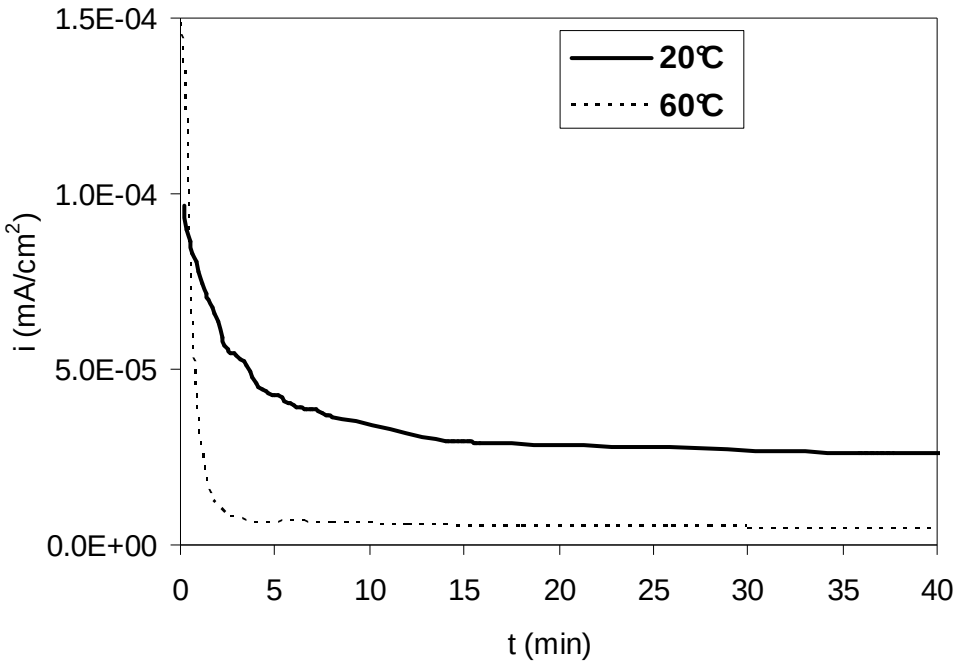

Figure 15 – Evolution of current density (with respect to defect areas) with time for freshly scratched coatings containing 30 % of dried organic agents exposed to a solution of NaCl-1 % at 20°C and 60°C under cathodic polarisation (-0.85 $V_{/Ag/AgCl}$).

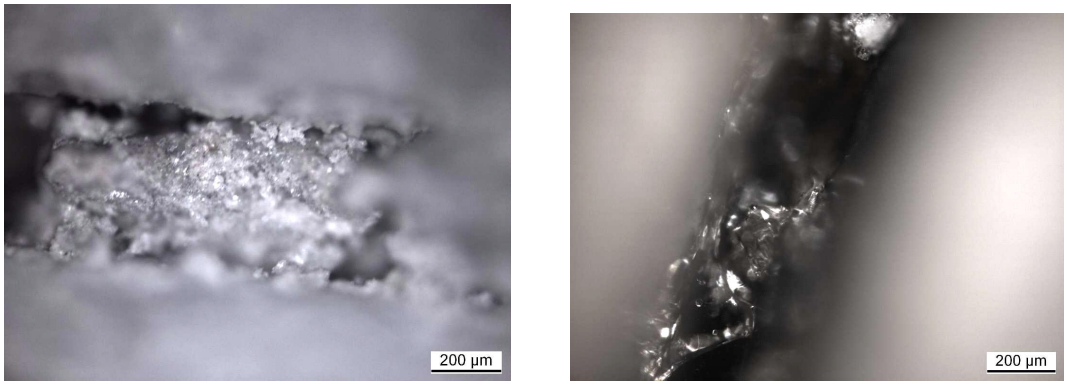

Figure 16 – Films deposited in a scratched coating area immersed in a solution of NaCl-1 % under cathodic polarisation (-0.85 $V_{/Ag/AgCl}$) during 40 hours: 20°C (left) ; 60°C (right).

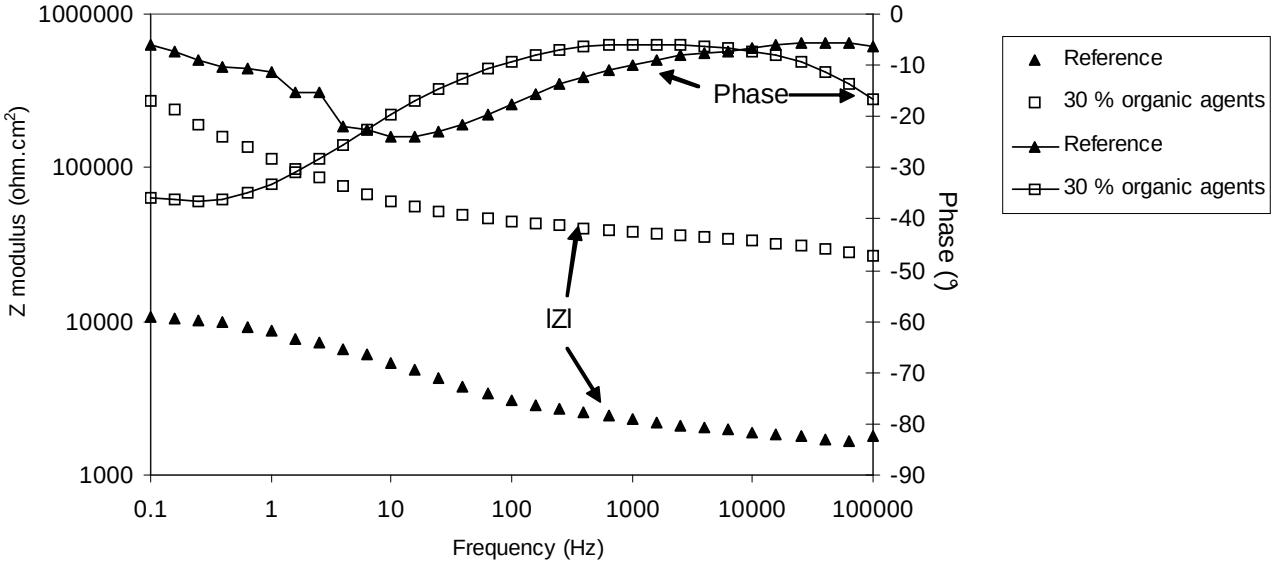

Figure 17 – Bode plots for scratched coatings exposed to a solution of NaCl-1 % at 20°C: reference (DFT = 200 µm, exposed area = 14 cm^2, defect area = 0.01 cm^2) and coating containing 30 % of organic film-formers exposed 40 hours to a solution of NaCl-1 % at 60°C under -0.85 $V_{/Ag/AgCl}$ CP and cured 15 days at ambient temperature (DFT = 800 µm, exposed area = 14 cm^2, defect area = 0.005 cm^2) .